

01 Jan 1989

## Characteristic Surfaces For Three-position Function Generation With Planar Four-bar Mechanisms

Clark R. Barker

*Missouri University of Science and Technology*

P. L. Tso

Follow this and additional works at: [https://scholarsmine.mst.edu/min\\_nuceng\\_facwork](https://scholarsmine.mst.edu/min_nuceng_facwork)

 Part of the [Mining Engineering Commons](#)

---

### Recommended Citation

C. R. Barker and P. L. Tso, "Characteristic Surfaces For Three-position Function Generation With Planar Four-bar Mechanisms," *Journal of Mechanical Design, Transactions of the ASME*, vol. 111, no. 1, pp. 104 - 109, American Society of Mechanical Engineers, Jan 1989.

The definitive version is available at <https://doi.org/10.1115/1.3258952>

This Article - Journal is brought to you for free and open access by Scholars' Mine. It has been accepted for inclusion in Mining Engineering Faculty Research & Creative Works by an authorized administrator of Scholars' Mine. This work is protected by U. S. Copyright Law. Unauthorized use including reproduction for redistribution requires the permission of the copyright holder. For more information, please contact [scholarsmine@mst.edu](mailto:scholarsmine@mst.edu).

# Characteristic Surfaces for Three-Position Motion Generation With Planar Four-Bar Mechanisms

C. R. Barker

Professor of Mechanical Engineering.  
Mem. ASME

J. Baumann

Graduate Student.

Mechanical and Aerospace Engineering  
Department,  
University of Missouri-Rolla,  
Rolla, MO 65401

*This paper considers the relationship between the three-position motion generation problem and the solution space for planar four-bar mechanisms. After one half of the basic four bar had been selected, two infinities of solutions still remained. These solutions are mapped in a plane to determine where the particular types of mechanisms occur. A contour is then generated in the mapping plane which joins together all solutions which share a common characteristic in regard to their link lengths. This same contour can be displayed in the solution space and in the Cartesian plane in which the motion generation is defined. Significant useful information to assist in selecting the final solution is obtained. A numerical example is used for illustration, but the results can be applied to any three-position motion generation problem.*

## Introduction

In the synthesis of planar four-bar mechanisms to satisfy a three-position motion generation problem, the designer is faced with choosing one solution from a very large number of potential solutions. In fact even if an initial choice is made for the location of one ground or moving pivot, two infinities of solutions still remain to complete the description of the mechanism. Information regarding the properties of this large body of solutions can be obtained by mapping in a plane the type of four bar which results for particular chosen parameters.

Harber, Erdman, and Riley [1, 2] have used this approach for the case of three prescribed positions by mapping the  $xy$ -plane into regions according to a classification scheme proposed by Barker [3]. After selecting one half of the four-bar mechanism, a map is generated which shows the influence of selecting the second half of the mechanism on the type which results. For each point selected in the  $xy$ -plane information is obtained concerning branching defects, toggling defects, minimum transmission angles, and maximum link length ratios.

The approach taken here is different from that of reference [1, 2] because an intermediate mapping plane called the  $\alpha\beta$ -plane will be used to generate all possible solutions to the synthesis problem. Then, the  $\alpha\beta$ -plane will be used to relate the  $xy$ -plane to the solution space [3] by generating a contour which joins together all solutions which have a common characteristic in regard to the lengths of their links. The advantage of this approach is that additional information is available to guide in the selection of the second half of the mechanism. As a result, it is easier to reject undesirable solutions rapidly and select an acceptable solution more quickly.

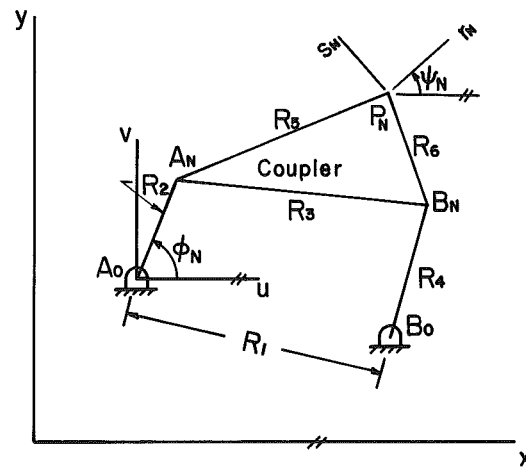


Fig. 1 Basic arrangement for three-position motion generation

The value of mapping the large number of solutions to the three-precision-point problem has been recognized by other researchers as well. Waldron and Strong [4] map areas corresponding to the rotation properties of links and joints of dyads using geometric techniques. Gupta [5] mapped areas where crank-rocker function generators exist and meet certain transmission angle requirements.

## Basic Arrangement

Figure 1 shows the basic arrangement for a three-position motion generation problem. The  $r_N s_N$ -axes are fixed to the coupler and move with it so that the origin  $P_N$  passes through three specified precision positions given in  $xy$ -coordinates by  $x_N y_N$  for  $N=1, 2$ , and  $3$ . At each precision position, the orientation of the  $r_N$ -axis relative to the  $x$ -axis is given by  $\psi_N$ .

The points  $A_0$  and  $B_0$  represent ground pivots (center points) whose locations are to be determined. The points  $A_N$

Contributed by the Mechanisms Committee and presented at the Design Engineering Technical Conference, Columbus, Ohio, October 5-8, 1985 of THE AMERICAN SOCIETY OF MECHANICAL ENGINEERS. Manuscript received at ASME Headquarters, July 1, 1986. Paper No. 86-DET-57.

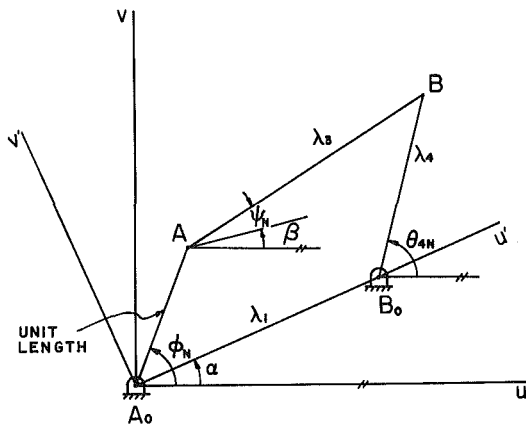


Fig. 2 Arrangement after first ground pivot has been selected

and  $B_N$  for  $N=1, 2$ , and  $3$  representing moving pivots (circle points) whose locations are also to be determined. Erdman and Sandor [6] discuss the number of free choices for this type of synthesis problem and the various strategies which may follow. One common strategy is to first select the location of one ground point, for example,  $A_0$  in Fig. 1.

Suppose this approach is taken and the vector

$$\bar{R}_{A_0} = x_{A_0} \hat{i} + y_{A_0} \hat{j} \quad (1)$$

is known as a result. Then it may be observed that since the position of  $P_N$  is known from the synthesis specifications, and the fact that  $A_N$  is a fixed point in the  $r_N s_N$  frame, it is true that

$$\bar{R}_{A_N/A_0} = \bar{R}_{P_N} + \bar{R}_{A_N/P_N} - \bar{R}_{A_0} \quad (2)$$

where

$$\begin{aligned} \bar{R}_{P_N} &= x_N \hat{i} + y_N \hat{j} \\ \bar{R}_{A_N/P_N} &= r_A \hat{r}_N + s_A \hat{s}_N \end{aligned}$$

and

$$\begin{aligned} \hat{r}_N &= \cos \psi_N \hat{i} + \sin \psi_N \hat{j} \\ \hat{s}_N &= -\sin \psi_N \hat{i} + \cos \psi_N \hat{j} \end{aligned}$$

Therefore

$$\begin{aligned} \bar{R}_{A_N/A_0} &= [x_N + r_A \cos \psi_N - s_A \sin \psi_N - x_{A_0}] \hat{i} \\ &+ [y_N + r_A \sin \psi_N + s_A \cos \psi_N - y_{A_0}] \hat{j} \quad \text{for } N=1,2,3 \end{aligned} \quad (3)$$

which leads to three equations in the unknowns  $r_A$ ,  $s_A$ , and  $R_2 = |\bar{R}_{A_N/A_0}|$ . It is thus a simple matter to solve for the required location of the moving pivot  $A_N$  in the coupler plane  $r_N s_N$  once the initial choice is made for the location of the ground pivot in the  $xy$ -plane. In addition, the three angles  $\phi_N$  which define the required orientation of the input link relative to the fixed  $xy$ -plane are also easily calculated at this point in the procedure.

Now consider the arrangement depicted by Fig. 2 where the basic four-bar link lengths have been normalized with respect to the input link length  $R_2$ . The three values of  $\phi_N$  and three values of  $\psi_N$  are known, but the angles  $\alpha$  and  $\beta$  are to be selected. Using a position vector loop equation with components taken in the  $u'v'$  system yields

$$\cos(\phi_N - \alpha) + \lambda_3 \cos(\psi_N + \beta - \alpha) = \lambda_1 + \lambda_4 \cos(\theta_{4N} - \alpha) \quad (4)$$

$$\sin(\phi_N - \alpha) + \lambda_3 \sin(\psi_N + \beta - \alpha) = \lambda_4 \sin(\theta_{4N} - \alpha).$$

Eliminating  $\theta_{4N}$  of the output link by squaring and adding leads to a result similar to that of Freudenstein [7] for the case of a three-position function generation problem where

$$K_1 \cos(\phi_1 - \alpha) + K_2 \cos(\psi_1 + \beta - \alpha) + K_3 = \cos(\psi_1 + \beta - \phi_1)$$

$$K_1 \cos(\phi_2 - \alpha) + K_2 \cos(\psi_2 + \beta - \alpha) + K_3 = \cos(\psi_2 + \beta - \phi_2) \quad (5)$$

$$K_1 \cos(\phi_3 - \alpha) + K_2 \cos(\psi_3 + \beta - \alpha) + K_3 = \cos(\psi_3 + \beta - \phi_3)$$

with

$$K_1 = \lambda_1 / \lambda_3, K_2 = \lambda_1$$

$$K_3 = (\lambda_4^2 - \lambda_1^2 - \lambda_3^2 - 1) / (2\lambda_3).$$

Using the notation

$$A_N = \cos(\phi_N - \alpha)$$

$$B_N = \cos(\psi_N + \beta - \alpha) \quad \text{for } N=1,2,3 \quad (6)$$

$$C_N = \cos(\psi_N + \beta - \phi_N)$$

it is possible to eliminate  $K_3$  from equation (5) and then solve for  $K_1$  and  $K_2$ . The result is

$$K_1 = \lambda_1 / \lambda_3 = \text{NUM1} / \text{DENOM} \quad (7)$$

$$K_2 = \lambda_1 = \text{NUM2} / \text{DENOM}$$

where

$$\text{NUM1} = (C_1 - C_2)(B_2 - B_3) - (C_2 - C_3)(B_1 - B_2)$$

$$\text{NUM2} = (C_2 - C_3)(A_1 - A_2) - (C_1 - C_2)(A_2 - A_3) \quad (8)$$

$$\text{DENOM} = (A_1 - A_2)(B_2 - B_3) - (A_2 - A_3)(B_1 - B_2).$$

The choice of  $\alpha$  and  $\beta$  will allow determining NUM1, NUM2, and DENOM from equation (8) and subsequently the values of  $\lambda_1$ ,  $\lambda_3$  and  $\lambda_4$  may be determined. Allowing  $\alpha$  and  $\beta$  to range from 0 to  $2\pi$  will cover all possible solutions to the motion generation problem for the initial choice made for the ground pivot location. A map in the  $\alpha\beta$ -plane can be constructed which shows the regions where a solution does exist.

The calculations are straightforward except for particular choices of  $\alpha$  and  $\beta$ . There are 12 special points where the equations become indeterminate because NUM1, NUM2, and DENOM are all zero. Let the values

$$\begin{aligned} \gamma_1 &= 1/2(\phi_1 + \phi_2) & \epsilon_1 &= 1/2(\psi_1 + \psi_2) \\ \gamma_2 &= 1/2(\phi_2 + \phi_3) & \epsilon_2 &= 1/2(\psi_2 + \psi_3) \\ \gamma_3 &= 1/2(\phi_3 + \phi_1) & \epsilon_3 &= 1/2(\psi_3 + \psi_1) \end{aligned} \quad (9)$$

be defined. Then when  $\alpha$  and  $\beta$  assume the values

$$\begin{aligned} \alpha &= \gamma_N & \beta &= \gamma_N - \epsilon_N \\ \alpha &= \pi + \gamma_N & \beta &= \gamma_N - \epsilon_N \\ \alpha &= \pi + \gamma_N & \beta &= \pi + \gamma_N - \epsilon_N \\ \alpha &= \gamma_N & \beta &= \pi + \gamma_N - \epsilon_N \end{aligned} \quad (10)$$

for  $N = 1, 2$ , and  $3$  the equation (7) becomes indeterminate. There is a relationship between the indeterminate points and the poles of the coupler motion. However, this topic requires further study and is beyond the scope of the present paper.

### Mechanism Mapping in the $\alpha\beta$ -Plane

It is desired that  $\lambda_1$ ,  $\lambda_3$ , and  $\lambda_4$  be positive and that  $\lambda = (\lambda_1 + \lambda_3 + \lambda_4) / \sqrt{3}$  be greater than  $\sqrt{3}/3$ . In order for this to be true, equation (7) shows that if DENOM  $> 0$  then NUM1 and NUM2 must also be greater than zero, or the reverse may occur where DENOM is negative and NUM1 and NUM2 must also be negative. The regions in the  $\alpha\beta$ -plane where these conditions are satisfied may be examined by finding the loci where NUM1, NUM2, and DENOM are zero.

**Locus of NUM1 = 0.** When NUM1 = 0, this corresponds to the condition that

$$(C_1 - C_2)(B_2 - B_3) = (C_2 - C_3)(B_1 - B_2). \quad (11)$$

If a value is chosen for  $\beta$ , then the  $C_N$  terms are known and it is possible to solve for the corresponding value of  $\alpha$ . The solution is

$$\tan \alpha = \frac{(C_2 - C_3)[\cos(\beta + \psi_1) - \cos(\beta + \psi_2)] - (C_1 - C_2)[\cos(\beta + \psi_2) - \cos(\beta + \psi_3)]}{(C_1 - C_2)[\sin(\beta + \psi_2) - \sin(\beta + \psi_3)] - (C_2 - C_3)[\sin(\beta + \psi_1) - \sin(\beta + \psi_2)]} \quad (12)$$

and for each value of  $\alpha$  found from equation (12)  $\pi$  may be added and subtracted and still provide a solution.

**Locus of NUM2 = 0.** The condition NUM2 = 0 is equivalent to

$$(A_2 - A_3)(C_1 - C_2) = (A_1 - A_2)(C_2 - C_3). \quad (13)$$

If a value is chosen for  $\alpha$ , the terms  $A_N$  are known and  $\beta$  can be solved for with the result that

$$\tan \beta = \frac{(A_1 - A_2)[\cos(\psi_2 - \phi_2) - \cos(\psi_3 - \phi_3)] - (A_2 - A_3)[\cos(\psi_1 - \phi_1) - \cos(\psi_2 - \phi_2)]}{(A_1 - A_2)[\sin(\psi_2 - \phi_2) - \sin(\psi_3 - \phi_3)] - (A_2 - A_3)[\sin(\psi_1 - \phi_1) - \sin(\psi_2 - \phi_2)]} \quad (14)$$

For each value of  $\beta$  found from equation (14), equation (13) is also satisfied if  $\pi$  is added or subtracted from  $\beta$ .

**Locus of DENOM = 0.** When DENOM = 0, it must also be true that

$$(A_1 - A_2)(B_2 - B_3) = (A_2 - A_3)(B_1 - B_2). \quad (15)$$

By assigning a value to  $\alpha$  the terms  $A_N$  are known and  $\beta$  is calculated from

$$\tan \beta = \frac{(A_2 - A_3)[\cos(\psi_1 - \alpha) - \cos(\psi_2 - \alpha)] - (A_1 - A_2)[\cos(\psi_2 - \alpha) - \cos(\psi_3 - \alpha)]}{(A_2 - A_3)[\sin(\psi_1 - \alpha) - \sin(\psi_2 - \alpha)] - (A_1 - A_2)[\sin(\psi_2 - \alpha) - \sin(\psi_3 - \alpha)]} \quad (16)$$

Once again, adding or subtracting  $\pi$  to the value of  $\beta$  will also satisfy equation (15).

### Numerical Example

In order to illustrate the generation of a map in the  $\alpha\beta$ -plane, a numerical example was chosen from reference [6, pp. 446-449]. In this example, the three-precision positions are defined by

$$\begin{array}{lll} x_1 = 0 & y_1 = 0 & \psi_1 = 0^\circ \\ x_2 = -6 & y_2 = 11 & \psi_2 = 22^\circ \\ x_3 = -17 & y_3 = 13 & \psi_3 = 68^\circ. \end{array} \quad (17)$$

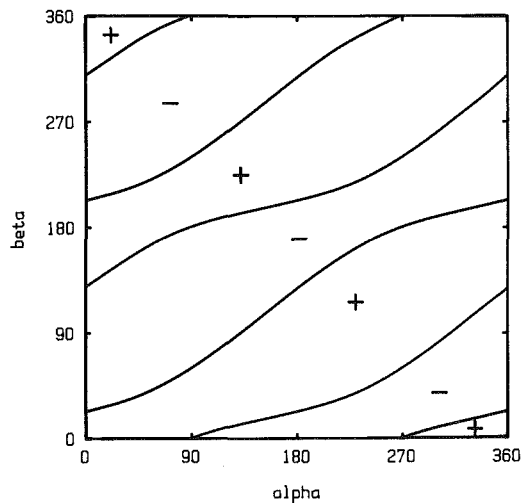


Fig. 3 Locus of NUM1 = 0 in  $\alpha\beta$ -plane

If the first ground pivot is chosen at the location

$$x_{A_0} = -20.3656 \quad y_{A_0} = 2.9889 \quad (18)$$

then equation (13) yields a solution where

$$\begin{array}{ll} r_A = -14.61056 \\ s_A = 3.46981 \\ R_2 = 5.77510. \end{array} \quad (19)$$

The corresponding positions of the input link specify that

$$\begin{array}{ll} \phi_1 = 4.777^\circ \\ \phi_2 = 94.777^\circ \\ \phi_3 = 202.777^\circ \end{array} \quad (20)$$

The values of  $\psi$  and  $\phi$  given in equations (17) and (20) were used in equation (12) to define the locus where NUM1 is zero for this numerical example. The result is shown in Fig. 3 and the positive and negative regions are labeled accordingly.

Figures 4 and 5 show the results of using the same data in equations (14) and (16). The positive and negative regions are indicated in the same fashion.

**Superposition of Regions.** Figures 3-5 can be used to construct an  $\alpha\beta$  map which shows the locations where a solution to the chosen numerical example exists. Since it is necessary for  $\lambda_1$ ,  $\lambda_3$ , and  $\lambda_4$  to all be positive, areas where NUM1, NUM2, and DENOM are all either positive or negative are to be added to one another. This process of superposition can be accomplished easily using computer graphics. Figure 6 shows a map in the  $\alpha\beta$ -plane for the problem defined in equations (17) and (18). The shaded regions correspond to  $\alpha\beta$  choices which produce positive  $\lambda_1$ ,  $\lambda_3$ , and  $\lambda_4$ . The locations of the 12

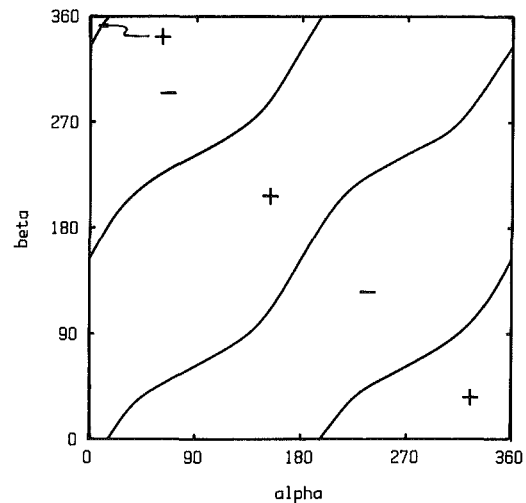


Fig. 4 Locus of NUM2 = 0 in  $\alpha\beta$ -plane

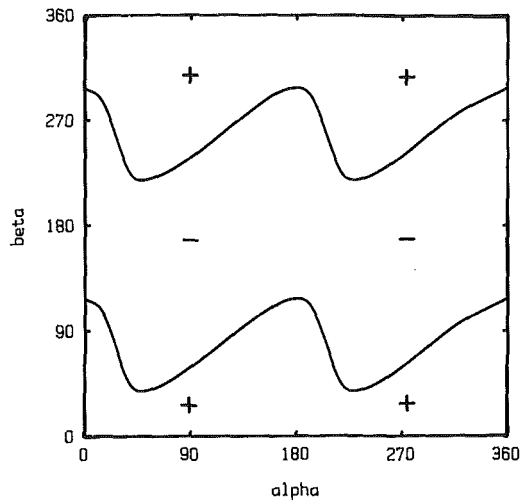


Fig. 5 Locus of DENOM = 0 in  $\alpha\beta$ -plane

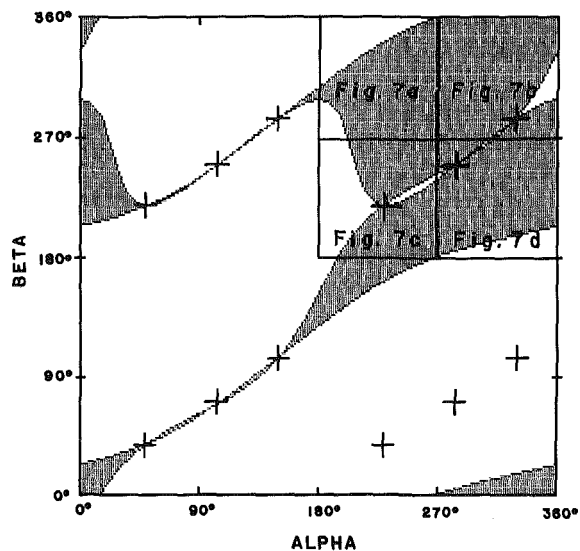


Fig. 6 Regions where a solution exists for numerical example

indeterminate points for this example were calculated using equations (9) and (10) and are shown in Fig. 6 by crosses. Note that three of the cross locations reside in an area where there was no solution and therefore they can be discarded. The six locations in the left half of Fig. 6 are in regions where the solution will be very sensitive to the choice of  $\alpha$  and  $\beta$  and consequently the mechanisms in these regions would be of little practical value. The remaining three indeterminate points, those in the top right half of Fig. 6, are in the region where the bulk of the potential solutions reside; that is, in the range  $180^\circ < \alpha < 360^\circ$  and  $180^\circ < \beta < 360^\circ$ . In order to illustrate the detail of this region, Fig. 7(a-d) were constructed. The darker regions correspond to locations where non-Grashof mechanisms are found and the lighter regions are where Grashof mechanisms are found. Most of the larger regions are labeled with the appropriate classification symbol from reference [3].

**Contours of Constant  $\lambda$ .** The influence of  $\alpha$  and  $\beta$  on determining the type of mechanism was illustrated in the last section. Each  $\alpha\beta$  pair chosen produces a corresponding location for the second ground pivot to go with the first ground pivot location defined in equation (18). We now address the question, which  $\alpha\beta$  pairs produce a second ground pivot loca-

Table 1 Comparison of possible solutions

Point	$B_0$ Location		Transmission Angle					
	$x, y$	$\lambda_1$	$\lambda_3$	$\lambda_4$	Max	Min		
$R_6$	-16.953, -5.293	1.551	3.220	3.184	46.9°	9.9°		
$A'$	-1.876, 3.848	3.205	1.698	3.050	122.1°	45.0°		
$D'$	-1.233, 3.151	3.313	1.707	2.934	135.0°	52.0°		
$E'$	-33.437, -10.967	3.311	1.762	2.880	135.0°	53.3°		
$F'$	-32.589, -10.453	3.147	1.801	3.004	117.1°	45.0°		

tion such that the link dimensions produce a specific value of  $\lambda$  where  $\lambda$  is defined by

$$\lambda = (\lambda_1 + \lambda_3 + \lambda_4) / \sqrt{3}. \quad (21)$$

The condition that  $\lambda$  be a chosen constant is equivalent to  $3K_1\lambda^2 - 2\sqrt{3}\lambda(K_1K_2 + K_2) + 2K_2^2 - 2K_2K_3 - K_1 = 0$  (22)

and by eliminating  $K_3$  and using equation (4), it is possible to show that

$$3\lambda^2(\text{NUM1})(\text{DENOM}) + 2(\text{NUM2})^2(1 - B_1)$$

$$- 2(\text{NUM2})(\text{DENOM})(\sqrt{3}\lambda - C_1) - (\text{NUM1})(\text{DENOM}) \quad (23)$$

$$- 2(\text{NUM1})(\text{NUM2})(\sqrt{3}\lambda - A_1) = 0.$$

Equation (23) contains only  $\alpha$ ,  $\beta$  and  $\lambda$  so that for a chosen  $\lambda$  it is possible to solve numerically for  $\alpha\beta$  pairs which satisfy equation (23). This procedure was followed to construct Fig. 8 where in this case the value  $\lambda = 4.592$  was selected (to agree with the example from reference [6]). Each point in Fig. 8 on the locus  $\lambda = 4.592$  corresponds to a particular point in the solution space and the  $xy$ -plane. Figures 9 and 10 are therefore derived from Fig. 8. Figure 10 shows the required locations of the second ground pivot  $B_0$  for the given choice of  $A_0$  that yields a  $\lambda = 4.592$ . Figure 9 shows the corresponding points in the solution space in the plane  $\lambda = 4.592$ .

## Discussion of Results

There are two separate branches shown in Figs. 8-10 labeled *ABCD* and *EFGH*. The points *A-H* are change points since, as shown in Fig. 9, they lie in the change point planes. This means that all the mechanisms between a particular pair of these points will be of the same type. Figure 9 shows that no *GCCC* solutions exist to this synthesis problem for the value of  $\lambda$  chosen. There will be *GCRR* solutions between *B* and *C*, *A* and *D*, *E* and *F*, and *G* and *H*. Applying this information to Fig. 10 shows the locations where the second ground point  $B_0$  may be chosen to produce *GCRR* solutions. The initial choice for  $A_0$  is shown also in Fig. 10 along with the design positions  $P_1$ ,  $P_2$ , and  $P_3$ .

Previous work on the solution space, reference [8], has shown that a zone of favorable transmission angles exists for *GCRR* and *GCCC* mechanisms. If, for example, it is desired that the transmission angle fall in the range  $45^\circ$  to  $135^\circ$ , then only those mechanisms in Fig. 9 between *A'* and *D'* and *E'* and *F'* need be considered. This is because at *D'* and *E'* the maximum transmission angle is  $135^\circ$  and at *A'* and *F'* the minimum transmission angle is  $45^\circ$ . At all locations in between, the range will satisfy the criteria specified. Locating these corresponding points in Fig. 10 shows that the satisfactory locations for the second ground point  $B_0$  are limited to a small zone for this  $\lambda$ -value.

The point  $R_6$  in Fig. 10 represents the location of  $B_0$  chosen in reference [6]. This location is far from the desired locations which provide a good range of transmission angle. Table 1 shows a comparison of the required link lengths, maximum and minimum transmission angles and required ground pivot locations for the solution of reference [6] and the four alternate solutions *A'*, *D'*, *E'* and *F'* found here.

The solution represented by *A'* and *D'* must be assembled

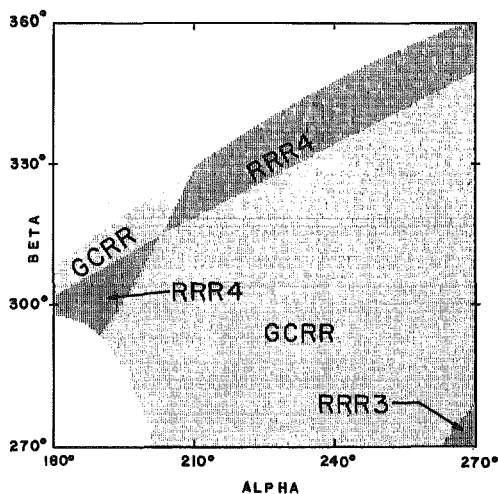


Fig. 7(a) Map of mechanism types for example

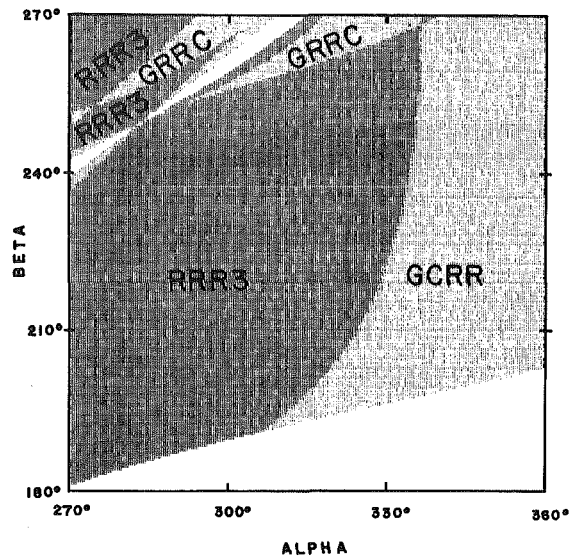


Fig. 7(d) Map of mechanism types for example

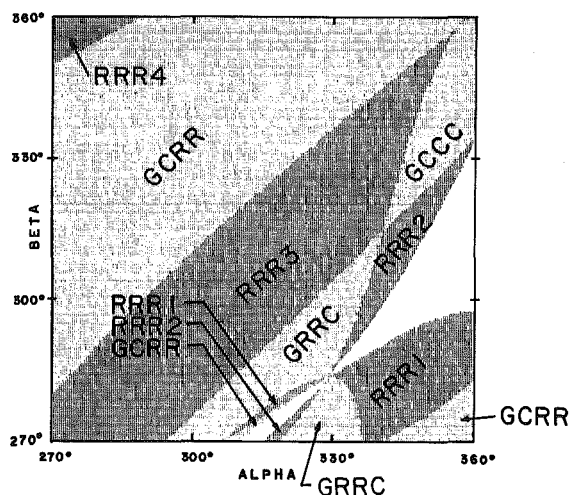


Fig. 7(b) Map of mechanism types for example

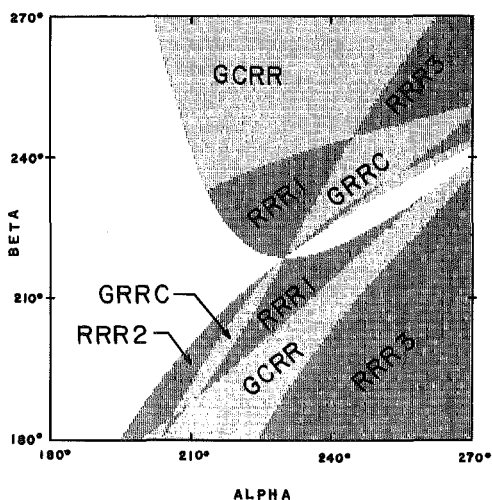


Fig. 7(c) Map of mechanism types for example

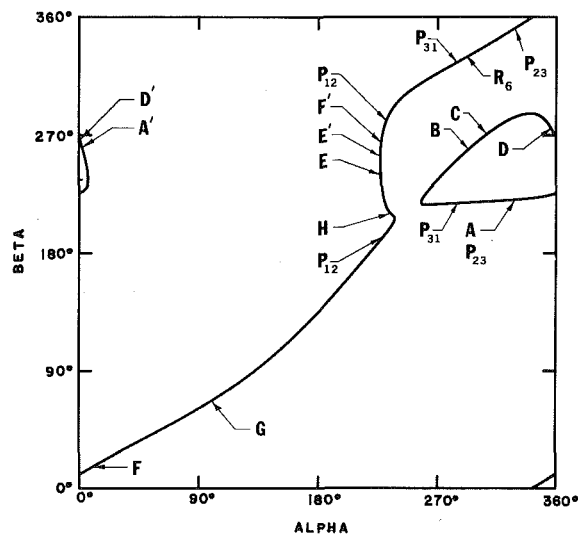


Fig. 8 Contour of  $\lambda = 4.592$  in  $\alpha\beta$ -plane

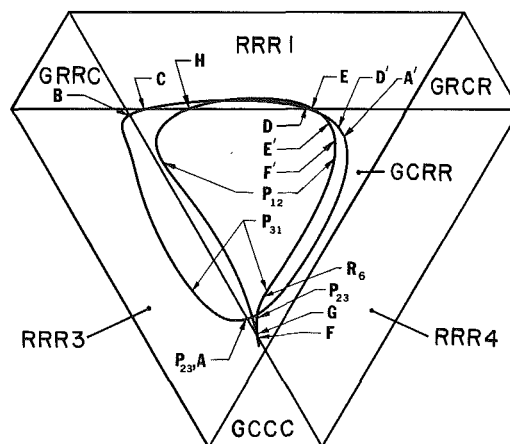


Fig. 9 Contour of  $\lambda = 4.592$  in solution space

in Form 2, reference [9], while those at  $R_6$ ,  $E'$ , and  $F'$  are to be assembled in Form 1.

Figure 10 also shows the location of the poles  $P_{12}$ ,  $P_{23}$ , and  $P_{31}$ . These locations correspond to a contour of constant  $\lambda$  intersecting itself or two different contours intersecting one another. The poles in the  $xy$ -plane appear as two separate

locations in the solution space, Fig. 9, and the  $\alpha\beta$ -plane, Fig. 8. However, both locations have the same value of  $\lambda_1$  and  $\alpha$ . These points are shown as  $P_{12}$ ,  $P_{23}$ , and  $P_{31}$  in Figs. 8 and 9. We may also observe that if a straight line is drawn in Fig. 10

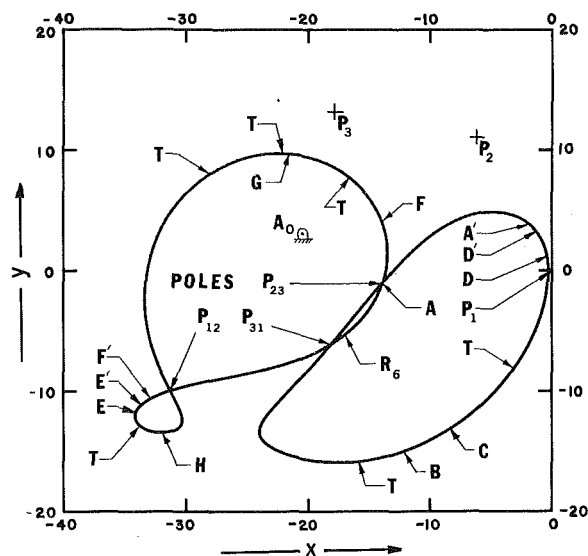


Fig. 10 Contour of  $\lambda = 4.592$  in  $xy$ -plane

between a pole and the point  $A_0$ , this straight line will intersect the contour at one of the indeterminant points (shown with symbol  $T$ ) predicted by equations (9) and (10). The full significance of these facts requires further study.

## Conclusion

The approach described here can be of considerable assistance in designing planar four-bar mechanisms for three-position motion generation synthesis. When the precision positions are selected, the  $\alpha\beta$ -plane can be used to map those regions where a solution will exist. The feasible regions may

further be subdivided into the locations where a particular type of four bar will be found. Contours of constant  $\lambda$  in the  $\alpha\beta$ -plane can be used to construct the locus of ground pivots in the  $xy$ -plane to provide a particular value of  $\lambda$ . This information yields the corresponding locus in the solution space which reveals where desirable mechanism solutions are found.

The development presented has employed a chosen numerical example for illustrative purposes. However, the approach is general and can form the basis for an interactive computer-aided synthesis program. The same technique can be applied as well to three-position function generation and path generation with prescribed timing.

## References

- 1 Harber, M. T., Erdman, A. G., and Riley, D. R., "Enhanced Computer Graphic Kinematic Synthesis for Three Prescribed Positions," *Proceedings of CAD/CAM, Robotics and Automation International Conference*, February 13-15, 1985, Tucson, AZ.
- 2 Harber, M. T., Erdman, A. G., and Riley, D. R., "Linkages Package Enhancements: A New Method for Three Design Position Synthesis," *Proceedings of the 9th Applied Mechanisms Conference*, October 28-30, 1985, Kansas City, MO.
- 3 Barker, C. R., "A Complete Classification of Planar Four-Bar Linkages," *Mechanism and Machine Theory*, Vol. 20, No. 6, 1985, pp. 535-554.
- 4 Waldron, K. J., and Strong, R. T., "Improved Precision Position Mechanism Synthesis," Report No. TR-12, Department of Mechanical Engineering, University of Houston, October 1978.
- 5 Gupta, K. C., "A General Theory for Synthesizing Crank-Type Four-Bar Function Generators With Transmission Angle Control," *ASME Journal of Applied Mechanics*, Vol. 45, No. 2, June 1968.
- 6 Erdman, A. G., and Sandor, G. N., *Mechanism Design: Synthesis and Analysis*, Vol. 1; Prentice-Hall, 1984, pp. 391-518.
- 7 Freudenstein, F., "An Analytical Approach to the Design of Four-Link Mechanisms," *Trans. ASME*, Vol. 76, 1954, pp. 483-492.
- 8 Barker, C. R., "Characteristic Surfaces in the Solution Space of Planar Four-Bar Mechanisms," Part 1 ASME Paper No. 84-DET-126, Part 2 ASME Paper No. 84-DET-127.
- 9 Barker, C. R., and Jeng, Y. R., "Range of the Six Fundamental Position Angles of a Planar Four-Bar Mechanism," *Mechanism and Machine Theory*, Vol. 20, No. 4, 1985, pp. 329-344.